Sol−Gel Template Synthesis of Semiconductor Oxide Micro- and Nanostructures

Brinda B. Lakshmi, Charles J. Patrissi, and Charles R. Martin*

Department of Chemistry, Colorado State University, Fort Collins, Colorado 80523

Received April 30, 1997. Revised Manuscript Received June 19, 1997[⊗]

The template method for synthesizing nanostructures involves the synthesis of the desired material within the pores of a nanoporous membrane or other solid. Our work has involved using porous alumina and polymeric filter membranes as the templates. Fibrils or tubules of the desired material are formed within each pore of the template membrane. A number of synthetic methods have been used to synthesize these nanostructures. This paper reviews sol−gel template synthesis: the use of sol−gel chemistry to synthesize semiconductor oxide micro- and nanostructures within the pores of micro- and nanoporous membranes. For example, TiO_2 nanotubules and nanofibers of the anatase form have been synthesized. The high surface area offered by these TiO_2 nanostructures has been used for photodecomposition of salicylic acid in sunlight. Enzyme immobilization by stannous bridges inside the TiO_2 tubes has also been studied. In addition, V_2O_5 fibrous electrode materials have been prepared by this method and Li intercalation electrochemistry is reported here. Other semiconductor oxides such as MnO_2, Co_3O_4, ZnO, WO_3, and SiO_2 have also been prepared.

Introduction

We have been exploring a general method for preparing nanomaterials which entails synthesis of the desired material within the pores of a nanoporous membrane or other solid.[1−3] The membranes used contain cylindrical pores with monodisperse diameters, and a nanoscopic fibril or tubule of the desired material is synthesized within each pore. This method has been used to make tubules and fibrils composed of polymers, metals, semiconductors, carbons, and Li-ion-intercalation materials.[1−3] Methods used to synthesize such materials within the pores of the template membranes include electroless metal deposition, electrochemical methods, and in situ polymerization.

Sol−gel chemistry has recently evolved as a powerful approach for preparing inorganic materials such as glasses and ceramics.[4−6] In sol−gel synthesis a soluble precursor molecule is hydrolyzed to form a dispersion of colloidal particles (the sol). Further reaction causes bonds to form between the sol particles resulting in an infinite network of particles (the gel). The gel is then typically heated to yield the desired material.[7] This method for the synthesis of inorganic materials has a number of advantages over more conventional synthetic procedures. For example, high-purity materials can be synthesized at a lower temperature. In addition, homogeneous multicomponent systems can be obtained by mixing precursor solutions; this allows for easy chemical doping of the materials prepared. Finally, the rheological properties of the sol and the gel can be utilized in processing the material, for example, by dip coating of thin films, spinning of fibers, etc.[6]

We have combined the concepts of sol−gel synthesis and template preparation of nanomaterials to yield a new general route for preparing nanostructures of semiconductors and other inorganic materials. This was accomplished by conducting sol−gel synthesis within the pores of various micro- and nanoporous membranes. Monodisperse tubules and fibrils of the desired material are obtained. Micro- and nanostructures of inorganic oxides such as TiO_2, MnO_2, V_2O_5, Co_3O_4, ZnO, WO_3, and SiO_2 have been prepared. Synthesis and possible applications of some of these template-synthesized materials are reviewed here.

Membranes Used

Template membranes used for the sol−gel synthesis of the micro- and nanostructures described here include porous alumina membranes and "track-etched" polycarbonate filters. The porous aluminas are prepared electrochemically from aluminum metal.[8] The pores are arranged in a regular hexagonal array, and pore densities as high as 10^{11} pores cm^{-2} can be achieved.[9] Membranes of this type with pore diameters of 200 nm are commercially available (Whatman, Anodisc). We have used these membranes in the studies described here. In addition, we have prepared membranes of this type with pore diameters as small as 10 nm.[10−12] An in-house prepared membrane with 22-nm-diameter

* Corresponding author. E-mail: crmartin@lamar.colostate.edu.

[⊗] Abstract published in *Advance ACS Abstracts,* August 15, 1997.

(1) Martin, C. R. *Science* **1994**, *266*, 1961.
(2) Martin, C. R. *Acc. Chem. Res.* **1995**, *28*, 61.
(3) Martin, C. R. *Chem. Mater.* **1996**, *8*, 1739.
(4) Brinker, C. J.; Scherer, G. W. *Sol−gel Science*; Academic Press Inc.: New York, 1990.
(5) Hench, L. L.; West, J. K. *Chem. Rev. (Washington, D.C.)* **1990**, *90*, 33.
(6) Aegerter, M. A.; Mehrota, R. C.; Oehme, I.; Reisfeld, R.; Sakka, S.; Wolfbeis, O.; Jorgensen, C. K. *Optical and electronic phenomena in Sol−Gel Glasses and Modern Applications*; Springer-Verlag: Berlin, 1996; Vol. 85.
(7) Livage, J.; Henry, M.; Sanchez, C. *Prog. Solid. State Chem.* **1988**, *18*, 259.
(8) Despic, A.; Parkhuitik, V. P. *Modern Aspects Of Electrochemistry*; Plenum: New York, 1989; Vol. 20.
(9) AlMawiawi, D.; Coombs, N.; Moskovits, M. *J. Appl. Phys.* **1991**, *70*, 4421.
(10) Foss, C. A.; Tierney, M. J.; Martin, C. R. *J. Phys. Chem.* **1992**, *96*, 9001.

S0897-4756(97)00268-8 CCC: $14.00

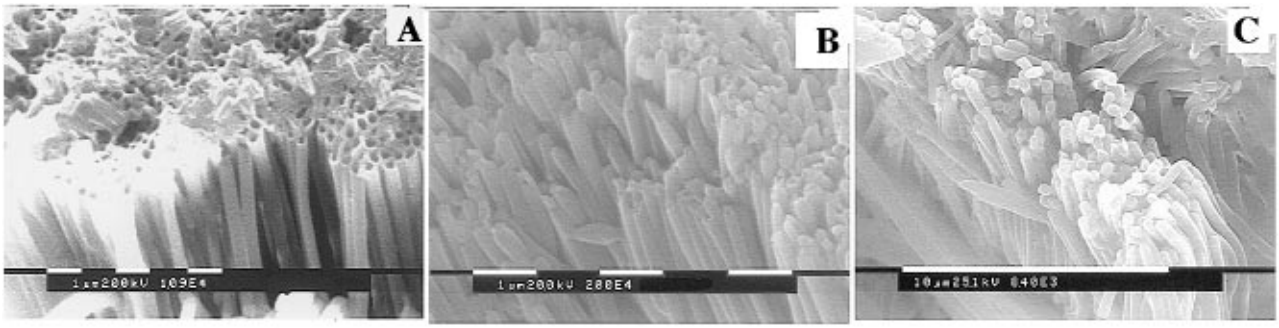

Figure 1. SEM image of TiO_2 nanostructures obtained by immersing the template membrane in the sol for (A) 5, (B) 25, and (C) 60 s.

pores was used in these studies. The "track-etch"[13] membranes are commercially available filters (Poretics). The pores in these membranes are randomly distributed across the membrane surfaces, and pore densities approaching 10^9 pores cm^{-2} can be obtained. A broad range of pore diameters (down to 10 nm) is available. We have used 600 nm pore diameter polycarbonate membranes of this type in this work.

Titanium Dioxide Nanostructures

Synthesis. Titanium isopropoxide was used as the precursor molecule for the sol−gel preparation of the TiO_2 nanostructures. The details of this synthesis are described elsewhere.[14] Briefly, the titanium isopropoxide is dissolved in 95% ethanol to yield a concentration of typically 20 v/v %. A second solution is then prepared by mixing 25 mL of ethanol with 0.5 mL of water and 0.5 mL of 0.1 M HCl. Equal volumes of the titanium isopropoxide solution and the second solution are then combined to yield the TiO_2 sol. The alumina template membrane is then dipped into this sol for the desired amount of time (see below), removed, and allowed to dry in air for 30 min. The sol-containing membrane is then heated in air at 400 °C for 24 h. This procedure yields TiO_2 tubules or fibrils within the pores and TiO_2 films on both faces of the template membrane. The surface films were removed by polishing the membrane with 1500 grit sand paper. If desired, the template membrane can then be dissolved away by immersion in aqueous base to expose the template-synthesized TiO_2 nanostructures.[14]

Figure 1 shows SEM images of TiO_2 tubules and fibrils prepared in the alumina membrane with 200-nm-diameter pores. Tubules were obtained if the membrane was immersed into the sol for a brief period (5 s, Figure 1a), whereas solid TiO_2 fibrils were obtained after long immersion times (60 s, Figure 1c). Intermediate immersion times yield tubules with very thick walls (25 s, Figure 1b). In all cases the tubules and fibrils were 50 μm long (the thickness of the alumina template membrane) and had an outside diameter of 200 nm (the diameter of the pores in the membrane).

Whether tubules or fibrils are obtained is also determined by the temperature of the sol. The structures shown in Figure 1 were obtained by immersion of the alumina template membrane into a sol maintained at 15 °C. When the sol was 5 °C, thin walled tubules were obtained even at long immersion times (1 min). In contrast, when the sol was maintained at 20 °C, solid TiO_2 fibrils were obtained even after very brief (5 s) immersion times. These results show that through control of temperature and immersion time, both tubules and fibrils can be prepared.

The mechanism of formation of TiO_2 from acidified titanium alkoxide solutions is well documented.[5,7] In the early stages, sol particles held together by a network of −Ti−O− bonds are obtained. These particles ultimately coalesce to form a three-dimensional infinite network, the gel. That tubules are initially obtained when this process is done in the alumina membrane indicates that the sol particles adsorb to the pore walls. It is well-known that at the pH values used here the sol particles are weakly positively charged.[15] In our prior paper[14] we suggested that tubules are formed because these positively charged particles interact with anionic sites on the alumina pore wall.

To explore this point further, we have recently conducted potentiometric experiments[16] on commercially available alumina membranes of this type that have 20-nm-diameter pores at one face. These experiments indicate that the pore walls are, in fact, weakly cationic.[17] This is in agreement with published results.[18] Hence, electrostatic interactions between the pore wall and the sol particles cannot be invoked to explain why tubules are produced in the pores of these membranes. An alternative explanation is that the sol particles form Ti−O−Al bonds by hydrolysis with Al−OH sites[18] on the pore wall. This issue of the mechanism of tubule formation in these membranes is a point that will need further exploration.

It is of interest to note, however, that the interaction of the sol particles with the alumina pore wall accelerates the rate of the gelation process. When a lower concentration of titanium isopropoxide (6 v/v % as opposed to the 20 v/v % used in Figure 1) was used to make the sol, gelation in bulk solution was extremely slow, even at room temperature. However, when the alumina membrane was dipped into this sol, solid fibrils of TiO_2 are obtained in the pores, even at short (5 s)

(11) Foss, C. A. J.; Hornyak, G. L; Stockert, J. A.; Martin, C. R. *Adv. Mater.* **1993**, *5*, 135.
(12) Foss, C. A. J.; Hornyak, G. L.; Stockert, J. A.; Martin, C. R. *J. Phys. Chem.* **1994**, *98*, 2963.
(13) Fleischer, R. L.; Price, P. B.; Walker, R. M. *Nuclear Tracks In Solids*; University of California Press: Berkeley, 1975.
(14) Lakshmi, B. B.; Dorhout, P. K.; Martin, C. R. *Chem. Mater.* **1997**, *9*, 857.
(15) Bischoff, B. L.; Anderson, M. A. *Chem. Mater.* **1995**, *7*, 1772.
(16) Nishizawa, M.; Menon, V. P.; Martin, C. R. *Science* **1995**, *268*, 700.
(17) Kobayashi, Y.; Lakshmi, B. B.; Martin, C. R.; unpublished results, June, 1997.
(18) Diggle, J. W.; Downie, T. C.; Goulding, C. W. *Chem. Rev.* **1969**, *69*, 365.

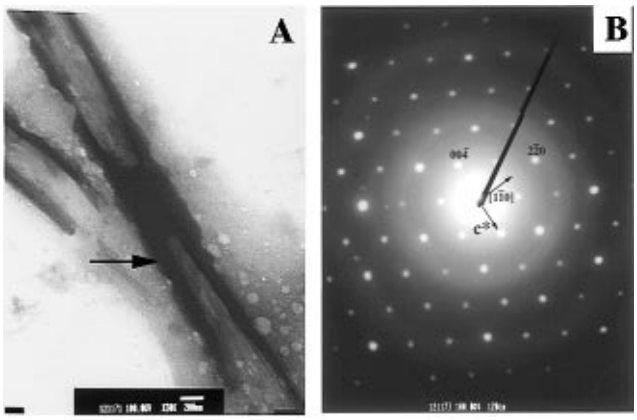

Figure 2. (A) TEM image of a bundle of 22-nm-diameter TiO_2 fibers. (B) Electron diffraction data for the fiber bundle in (A).

immersion times. These results show that gelation occurs within the pores under conditions where gelation in bulk solution is negligibly slow.

Electron Diffraction. Figure 2a shows a transmission electron microscopic (TEM) image of the TiO_2 nanostructures synthesized in the alumina membrane with 22-nm-diameter pores. After synthesis, the template membrane was dissolved, and the TiO_2 fibers were collected on a TEM grid. Numerous images of this type were obtained, and in all cases bundles of the 22-nm-diameter TiO_2 nanostructures were observed. The bundle sizes observed ranged from as small as 2−4 fibrils to as large as 10 or more fibrils.

Figure 2b shows the indexed electron diffraction pattern obtained from such a fibril bundle. The orientation of the images in Figures 2a,b are the same; that is, the c* axis in Figure 2b is parallel to the fibril bundle axis in Figure 2a. These data show that the fibrils are highly crystalline anatase-phase TiO_2, with the c* axis of the anatase oriented along the long axis of the fibril. Small fibril bundles throughout the sample displayed the same crystalline orientation; i.e., the reciprocal lattice direction [110] is almost always parallel to the electron beam, and the c* axis is along the fibril axis.

We can conclude from these observations that the fibrils crystallize as long, prismatic crystals with the rare, and metastable, anatase mineralogical orientation [001] with {110}.[19] It is of interest to note that small fibril bundles do not show a great deal of mosaic spread in the diffracted electron beam, as one would expect for polycrystalline materials or oriented polymer fiber samples. Larger bundles of crystalline fibrils do show mosaic spreading of the reflections, but they remain oriented along their [001] fiber axis. For example, bundles with diameters as large as 1 μm and lengths corresponding to the entire thickness of the template membrane (in this case 30 μm) are single crystals.

Sol−gel synthesis can result in crystallization of metastable phases because of the low-temperature preparation.[20] It is also known that sol−gel synthesis can yield single-crystalline material at low temperature.[21] Finally, electron diffraction data from the 200 nm diameter TiO_2 fibrils show that these fibrils are also highly crystalline anatase.[14] However, the data suggest that these larger-diameter fibrils are not single crystals.

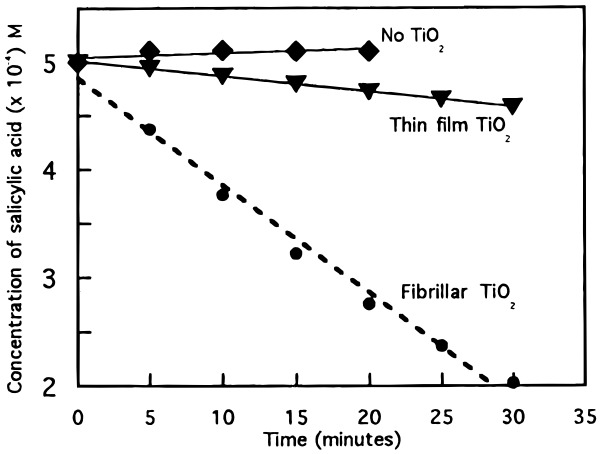

Figure 3. Photodecomposition of 15 mL of 0.5 mM salicylic acid in sunlight. Upper curve: no photocatalyst. Middle curve: thin-film TiO_2 catalyst. Lower curve: fibrous TiO_2 catalyst.

Photocatalysis. TiO_2 is a semiconductor with a large bandgap of 3.2 eV. The phocatalytic and photoelectrochemical properties of TiO_2 are well documented.[22] When exposed to UV light of energy greater than the bandgap, electrons are excited to the conduction band forming electron−hole pairs. These react with water to yield hydroxyl and superoxide radicals which are good oxidizing agents. This makes TiO_2 an excellent photocatalyst for the decomposition of organic pollutants.[23,24]

TiO_2 exists in more than one form; the important phases being rutile and the metastable anatase.[25] Anatase has been found to be the best phase for photocatalysis.[25] It has been shown that high surface area anatase allows for greater photocatalytic efficiency.[26] For this reason, suspensions of anatase powder have been investigated as possible photocatalysts.[24,25] However, such suspensions are difficult to handle, and sampling to determine the photocatalytic efficiency requires separation of the particles from the solution. The ideal system would be to immobilize a high surface area anatase catalyst on a solid support. Sol−gel template synthesis allows us to prepare such a high surface area immobilized TiO_2 photocatalyst.[14]

The catalyst investigated was an ensemble of 200-nm-diameter TiO_2 fibers that protrude from an epoxy surface like the bristles of a brush (Figure 1C). Aqueous solutions of salicylic acid were used to explore the photodecomposition efficiency of this catalyst. Sunlight was used as the light source.[14] Figure 3 shows plots of salicylic acid concentration vs time of exposure to sunlight. The upper curve is for a solution that contained no photocatalyst, and no decomposition of salicylic acid is observed. The middle curve is for a sol−gel synthesized thin film TiO_2 photocatalyst; catalytic decomposition of salicylic acid is now observed. However, the rate

(19) Dana, J. D. Rewritten by: Polache, C.; Berman, H.; Frondel, C. *The system of mineralogy*; John Wiley: New York, 1955.
(20) Lange, F. F. *Science* **1996**, *273*, 903.
(21) Spanhel, L.; Anderson, M. A. *J. Am. Chem. Soc.* **1991**, *113*, 2826.
(22) Fujishima, A.; Honda, K. *Nature* **1972**, *37*, 238.
(23) Matthew, R. W. *J. Phys. Chem.* **1987**, *91*, 238.
(24) Kraeutler, B.; Bard, A. J. *J. Am. Chem. Soc.* **1978**, *100*, 5985.
(25) Linsebigler, A. L.; Lu, G.; Yates, J. T. *Chem. Rev. (Washington, D.C.)* **1995**, *95*, 735.
(26) Yoko, T.; Yuasa, A.; Kamiya, K.; Sakka, S. *J. Electrochem. Soc.* **1991**, *138*, 2279.

of decomposition is an order of magnitude lower than for the fibrillar TiO_2 photocatalyst (Figure 3).[14]

The increase in the decomposition rate observed with the TiO_2 fibers is due to their higher surface area (relative to the thin film). A 1 cm^2 area of thin film was used. The area of the epoxy support for the fibrillar catalyst was also 1 cm^2, but the total surface area of the TiO_2 fibrils protruding from this catalyst is ~315 cm^2. Given this dramatically higher surface area, it is surprising that an enhancement in photodecomposition rate of only 1 order of magnitude is observed. This is because, as shown in Figure 1, the TiO_2 fibers lean against each other and thus shade each other from the incident sunlight. This suggests that an optimum length and density of fibers must be identified so as to maximize the surface area of the fibers exposed to the light. Finally, quantitative analysis on the rate of decomposition shows pseudo-first-order kinetics with a rate constant of 0.03 min^{-1} for the fibers as opposed to 0.003 min^{-1} for thin film.[14]

Enzyme Immobilization. The high surface areas of the template-synthesized nanostructures might also be advantageous in the area of enzyme immobilization to make bioreactors.[27] It has been shown that enzymes can be bound to TiO_2 surfaces using Sn^{2+} as a chemical linking agent.[28,29] This chemistry (eqs 1 and 2) links −SH groups from the enzyme to oxygen sites on the TiO_2 surface.

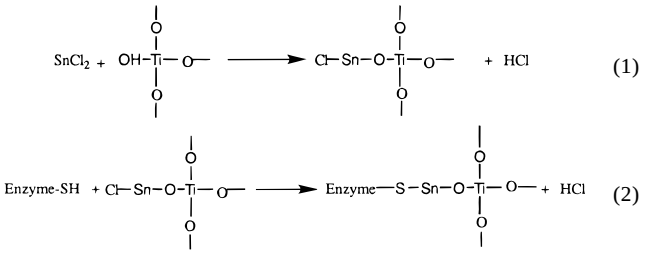

We have used this method to immobilize alcohol dehydrogenase to the inside walls of template-synthesized TiO_2 tubules such as those shown in Figure 1A. This was accomplished by first immersing the tubule-containing membrane into a solution of Sn^{2+} (1% aqueous $SnCl_2$) for 1 h to attach Sn^{2+} to the inner tube walls. The membrane was washed with distilled water and immersed into a solution of the alcohol dehydrogenase (1 mg of enzyme in 5 mL of water) overnight. The membrane was then washed with water several times before testing for the activity of the immobilized enzyme.

To show that the immobilized enzyme retains its catalytic activity the tubule-containing membrane (enzyme within the tubes) was immersed into a solution containing ethanol and the enzyme's soluble cofactor NAD^+. This solution was prepared by mixing 0.2 mL of 95% ethanol, 0.2 mL of 0.2 M NAD^+, 1 mL of pH 8.8 pyrophosphate buffer, and 1 mL of water. The course of the enzymatic oxidation of ethanol was monitored by measuring NADH absorbance at 340 nm (Figure 4). We have found that the enzyme immobilized in this way remains active for a minimum of 4 days.

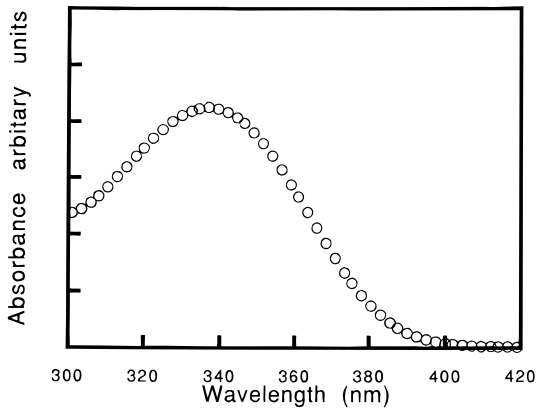

Figure 4. UV−vis spectrum showing the NADH absorption at 340 nm resulting from alcohol dehydrogenase-catalyzed oxidation of ethanol.

In this experiment, the tubules remained within the pores of the template membrane, and the enzyme was immobilized on the inside walls of the tubes. Since both ends of the tubes are open, this configuration raises the possibility of making a flow-through bioreactor membrane. Substrate solution could be flowed through such a membrane, with bioconversion to product occurring while the solution is in transit through the tubes. The product of the enzymatic reaction would then be collected as the effluent from the membrane. Alternatively, the template membrane could be dissolved away leaving a high surface area ensemble of tubes protruding from a surface. Enzyme could then be immobilized on both the inner and outer walls of these tubes. We are currently investigating both of these types of bioreactors.

Manganese Dioxide Nanostructures

MnO_2 exists in a number of structural forms. The β-MnO_2 and ramsdellite are relatively pure forms of MnO_2.[30] Other forms, such as α, δ, and γ, contain ions such as Li^+, Na^+, and K^+ within the lattice. The basic building block consists of MnO_6 octahedra forming layers and channels.[30,31] These channels are large enough to intercalate Li^+ ions; as a result MnO_2 has been used as a Li-ion battery electrode material.[32] In addition, MnO_2 is also used in primary cells; for example, the commercial Zn−MnO_2 alkaline batteries utilize MnO_2 as the cathode material.

A number of synthetic methods are known for the preparation of MnO_2 cathodes. The cathodes for the commercial batteries are 1−2-mm-thick films which are synthesized electrochemically. The discharge performance of these batteries improve with higher cathode surface area.[33] The electrochemically prepared thin films do not have high surface area. Thin films of MnO_2 prepared by the sol−gel-route show better discharge performance and lower degradation rate.[32,34,35] This has

(27) Woodward, J. *Immobilized cells and enzymes*; IRL Press: Oxford, 1985.
(28) Kennedy, J. F.; Cabral, J. M. S. *Solid Phase Biochemistry*; John Wiley & Sons: New York, 1983; Vol. 66.
(29) Messing, R. *Methods of Enzymology*; Academic Press: New York, 1976; Vol. 44, p 148.
(30) Post, J. E.; Von Dreele, R. B.; Buseck, P. R. *Acta Crystallogr.* **1982**, *B38*, 1056.
(31) Hunter, J. C. *J. Solid. State Chem.* **1981**, *39*, 142.
(32) Le Goff, P.; Baffier, N.; Bach, S.; Pereira-Ramos, J. *J. Mater. Chem.* **1994**, *4*, 875.
(33) Yamamura, K.; Mizutani, M.; Ishikawa, R.; Miyashita, T.; Chiba, N.; Maeda, M. *Prog. Batt. Batt. Mater.* **1991**, *10*, 56.
(34) Stadniychuk, H. P.; Anderson, M. A.; Chapman, T. W. *J. Electrochem. Soc.* **1996**, *143*, 1629.
(35) Bach, S.; Henry, M.; Baffier, N.; Livage, J. *J. Solid. State Chem.* **1990**, *88*, 325.

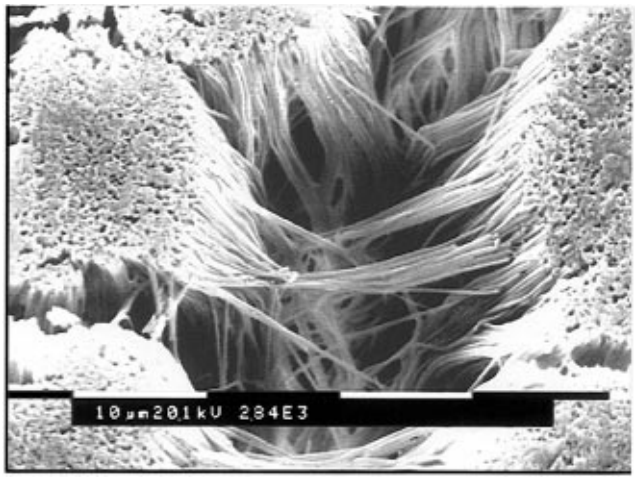

Figure 5. SEM image of MnO_2 fibers prepared in the 200-nm-pore-diameter alumina template membrane.

been attributed to the high surface area of the sol−gel synthesized material.[34] Because of the superior performance of the sol−gel-prepared material, and because it is clear that high surface is important, it seemed likely that sol−gel-synthesized nanostructures might be the ideal electrode material. For this reason we have used the template to prepare such MnO_2 nanostructures.

Potassium permanganate was used as the inorganic precursor and fumaric acid as the reducing agent.[34,35] Best results were obtained by mixing 0.7 g of fumaric acid with 3.8 g of $KMnO_4$, adding 2 mL of 2.5 M H_2SO_4, and then adding 100 mL of water. The resulting solution was stirred, and the course of the reaction was monitored by the color which changed from purple, to orange, to brown (∼10 min). The alumina membrane was then dipped for 10 s into this sol, removed, dried in air for 30 min, and then heated in air at 500 °C for 24 h. The surface MnO_2 layers on either face of the membrane were removed as before using 1500 grit sand paper. The membrane was then fixed onto an epoxy surface and the alumina template was dissolved using 6 M NaOH. This yielded an ensemble of MnO_2 fibers protruding from the substrate epoxy surface (Figure 5).

Electron diffraction data were obtained on these fibers in order to determine the phase of the MnO_2 prepared. This was accomplished by placing the fiber-containing membrane on a TEM grid and dissolving the membrane in aqueous base. A TEM image of a portion of a fiber obtained in this way is shown in Figure 6A. The electron diffraction pattern obtained from this fiber is shown in Figure 6B. This pattern shows discontinuous rings that were indexed to the α phase of MnO_2. The fact that these rings are discontinuous suggests that the crystalline domains that make up this fiber show some degree of preferred orinentation. We are currently investigating this point further. The use of such template-synthesized MnO_2 nanostructures as battery electrodes is also being investigated.

Vanadium Pentoxide Microstructures

V_2O_5 also shows reversible Li^+ intercalation and is of interest as a possible electrode material for Li-ion batteries and electrochromic devices.[36,37] One problem

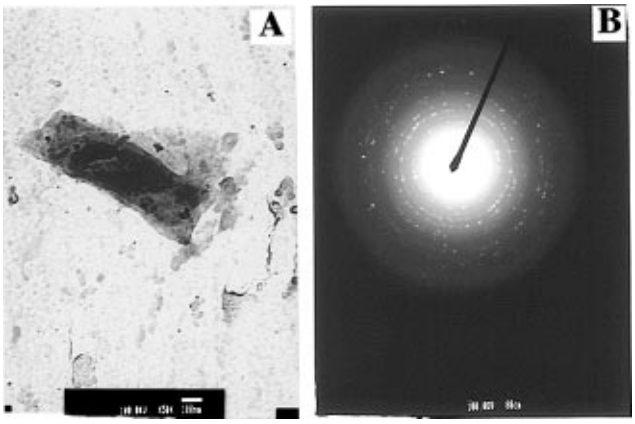

Figure 6. (A) TEM image of an MnO_2 fiber. (B) Electron diffraction data for the fiber in (A).

with V_2O_5 and other Li^+-intercalation materials, however, is that their rate capability is limited by the slow diffusion of Li^+ within the solid electrode material.[38] We are attempting to solve this problem by using the template approach to prepare nanostructured battery electrodes of this type.[39,40] Since it is well-known that V_2O_5 can be prepared via sol−gel methods,[41,42] sol−gel template synthesis seems like an attractive route for preparing such nanostructured electode materials.

The nanofibrous V_2O_5 electrodes were prepared using vanadium (V) triisopropoxy oxide (VTIP) as the precursor molecule. The 600-nm-pore-diameter polycarbonate filter was used as the template membrane. The template membrane was first placed onto the surface of a Ni wafer, which will serve as the current collector (2 × 3 × 0.1 cm, 99.9% Ni). In an argon atmosphere, the liquid VTIP was then applied to the surface of the template membrane. Because of its relatively low viscosity, the VTIP floods the pores and also fills the interface between the Ni foil and the membrane. The VTIP was then hydrolyzed by simply exposing the membrane to air with ambient humidity at 60 °C. After air exposure for 2 h, the template membrane was removed by exposure to an oxygen plasma. Finally, alkoxy ligand removal and condensation were effected by heating at 400 °C in air for 24 h.

Scanning electron microscope (SEM) images of the resulting material are shown in Figure 7. The low-magnification image (Figure 7A) shows that the V_2O_5 fibers are protruding from a V_2O_5 surface film formed at the interface between the template membrane and the underlying Ni current collector. The higher magnification image (Figure 7B) more clearly shows the monodisperse V_2O_5 fibrils that were formed within the pores of the template membrane. Preliminary X-ray diffraction data indicate that this material is crystalline α phase of V_2O_5.

Cyclic voltammetry was used to explore reversible Li^+ intercalation within this material. Voltammetry was performed under an argon atmosphere in a three-

(36) Delmas, C.; Cognac-Auradou, H.; Cocciantelli, J. M.; Menetrier, M.; Doumerc, J. P. *Solid State Ionics* **1994**, *69*, 257−264.
(37) Bates, J. B.; Gruzalski, G. R.; Dudney, N. J.; Luck, C. F.; Yu, X. *Solid State Ionics* **1994**, *70/71*, 619−628.
(38) Scrosati, B. *J. Electrochem. Soc.* **1992**, *139*, 2776−2781.
(39) Nishizawa, M.; Mukai, K.; Kuwabata, S.; Martin, C. R.; Yoneyama, H. *J. Electrochem. Soc.*, in press.
(40) Che, G.; Jirage, K. B.; Fisher, E. R.; Martin, C. R. *J. Electrochem. Soc.*, submitted.
(41) Davies, A.; Hobson, R. J.; Hudson, M. J.; Macklin, W. J.; Neat, R. J. *J. Mater. Chem.* **1996**, *6*, 49−56.
(42) Livage, J. *Solid State Ionics* **1996**, *86−88*, 935−942.

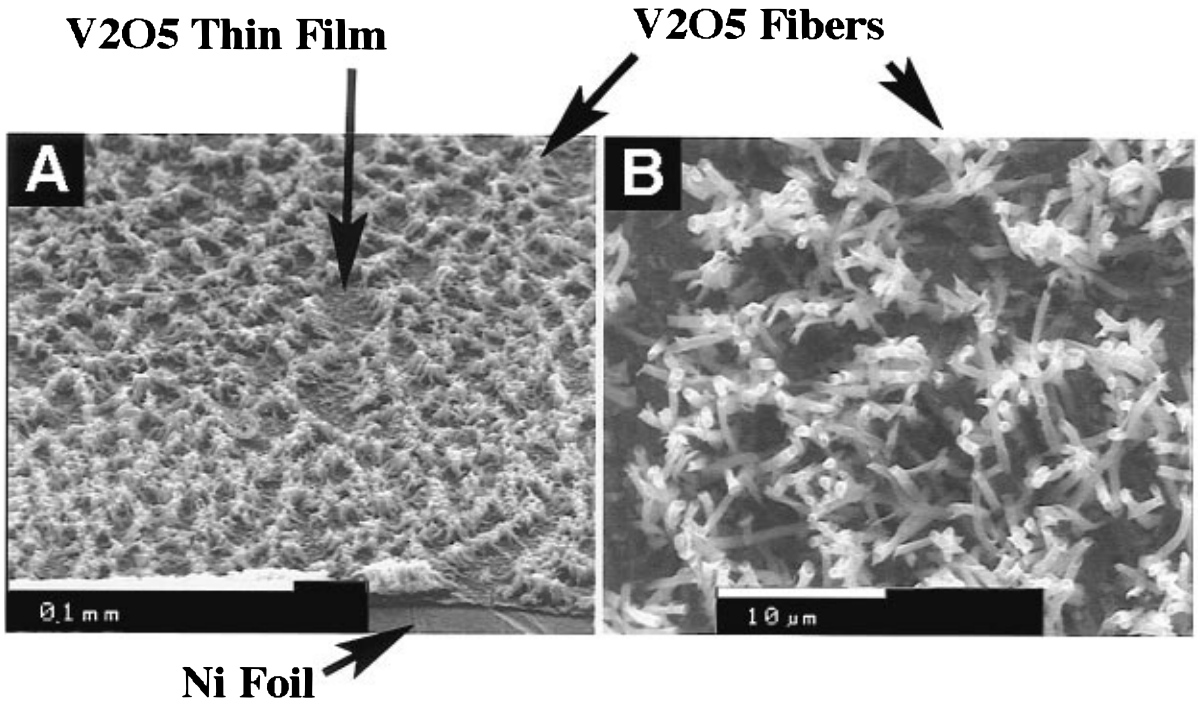

Figure 7. SEM images of the template-synthesized V_2O_5 microstructures.

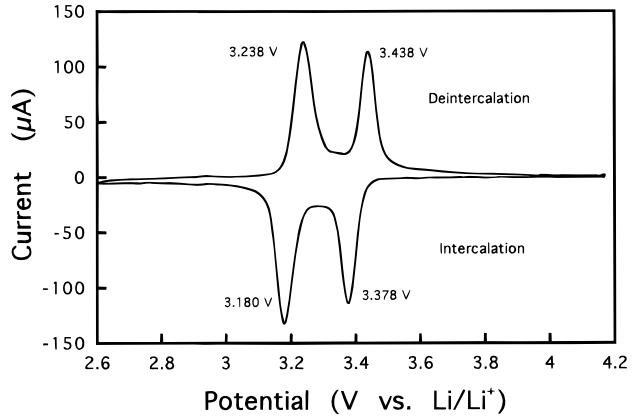

Figure 8. Cylic voltammogram showing the intercalation and deintercalation of Li^+ in the nanostructured V_2O_5 electrode.

electrode cell using the V_2O_5 (on Ni) as the working electrode and Li counter and reference electrodes. Voltammetric data were acquired by scanning at 0.10 mV s^{-1} between voltage limits of 4.17 and 2.60 V (vs Li/Li^+). The starting (and ending) potential was 4.17 V. The electrolyte was 1 M $LiClO_4$ in a 70:30 (w/w) mixture of diethyl carbonate and ethylene carbonate.

A typical voltammogram for the microstructured V_2O_5 electrode is shown in Figure 8. The peaks in the voltammogram indicate that Li^+ intercalation causes a phase change in the V_2O_5.[43] Analogous results were observed previously using the galvanostatic intermittent titration method.[36] The forward peak maxima observed in Figure 8 (3.4 and 3.2 V vs Li/Li^+) agree quite well with the plateau potentials observed in the galvanostatic intermittent titration data. The reversibility of the Li^+ insertion reaction is demonstrated here by the nearly equivalent areas under the intercalation (forward) and deintercalation (reverse) voltammetric waves. We are currently conducting charge−discharge experiments to explore the rate capabilities of these microstructured V_2O_5 electrodes.

Cobalt Oxide Nanostructures

Co_3O_4 has the spinel structure with cobalt existing in both the Co(II) and Co(III) valence states. This makes these materials excellent catalysts for carbon monoxide oxidation.[44] It seemed likely that sol−gel template-synthesized Co_3O_4 nanostructures might be useful as high surface area catalysts of this type.

Cobalt oxide nanofibers were prepared using $Co(NO_3)_2$ as the precursor material.[45] A solution that was 0.3 mM in Co^{2+} and 0.05 mM in citric acid was employed. This solution was allowed to hydrolyze for 1 h to produce the sol, and the alumina template membrane was immersed in this sol for 10 s. The membrane was then removed from the sol, allowed to dry in air for 30 min, and then heated in air at 500 °C for 24 h.

SEM images were obtained, as before, by fixing the membrane to an epoxy surface and then dissolving the membrane in aqueous base. A typical SEM image showing the monodisperse Co_3O_4 fibers obtained is shown in Figure 9. Fibers were also collected for TEM and electron diffraction analysis. A TEM image of a single Co_3O_4 fiber is shown in Figure 10A. Interestingly, while the SEM images suggest that these are continuous fibers with reasonable mechanical strength, the TEM images show that these fibers are, in fact, microporous. Longer sintering times (up to 48 h) did not remove this microporosity. The corresponding electron diffraction pattern shows continuous rings

(43) McKinnon, W. R. In *Solid-state electrochemistry*; Bruce, P. G.; Ed.; Cambridge University Press: Cambridge, 1995; pp 163−197.

(44) Omata, K.; Takada, T.; Yamada, M. *Appl. Catal. A, General* **1996**, *146*, 255.

(45) Zhecheva, E.; Stoyanova, R.; Gorova, M.; Alcantara, R.; Morales, J.; Tirado, J. L. *Chem. Mater.* **1996**, *8*, 1429.

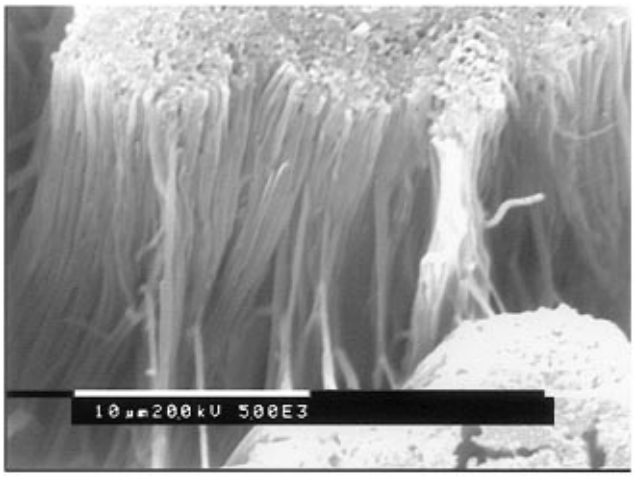

Figure 9. SEM image of Co_3O_4 fibers prepared in the 200-nm-pore-diameter alumina template membrane.

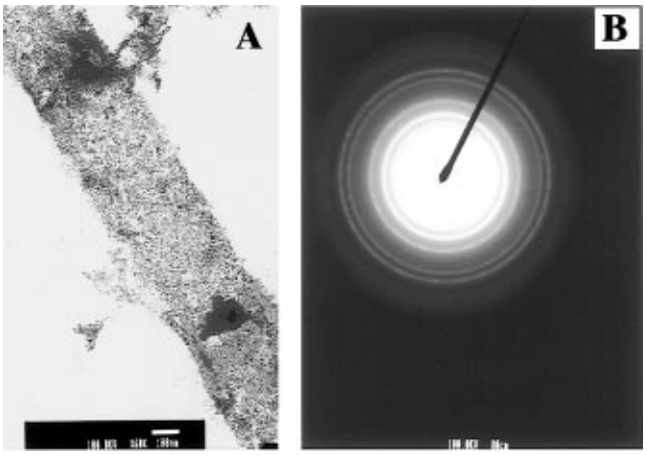

Figure 10. (A) TEM image of a Co_3O_4 fiber. (B) Electron diffraction data for the fiber in (A).

which were indexed to the spinel Co_3O_4 (Figure 10B). The rings are sharp and continuous, which shows that although the fibers are highly crystalline, they are not single crystals, and the various crystalline domains show no preferred orientation.

Other fibers such as ZnO, WO_3,[14] and SiO_2 have been prepared by this sol−gel route. The applications for these fibers are being investigated.

Conclusion

Sol−gel synthesis has been used to make oxide nanostructures via the template method. These nanostructures offer very high surface area due to the high porosity of the template membranes employed. Synthetic conditions could be controlled for TiO_2 such that both nanotubes and nanofibers could be obtained. The TiO_2 nanofibers show increased rate of photodecomposition of salicylic acid. This is attributed to the high surface area offered by these nanostructures. Enzyme immobilization in the TiO_2 tubes through stannous bridge chemistry has also been accomplished. In addition, micro and nanostructured battery-electrode materials such as MnO_2 and V_2O_5 have been prepared. The effect of fiber dimensions on the rate capabilities of alkaline and Li-ion batteries using these MnO_2 and V_2O_5 nanofibrous electrodes is being investigated. Nanofibers of other catalysts such as Co_3O_4, ZnO, WO_3,[14] and SiO_2 have also been prepared.

Acknowledgment. This work was supported by the Office of Naval Research, the National Science Foundation and the Department of Energy.

CM970268Y